

ures by error bars. Heat haze was not an obvious problem, even over our longest sightings (350 m) on the hottest days, perhaps because a gentle breeze was usually blowing.

8. C. J. Talbot, *J. Struct. Geol.* 1, 5 (1979).
9. On both occasions the surface of the salt glacier dried thoroughly, the colors paled, and white salt was reprecipitated along the grain boundaries on most exposed surfaces. On humid or wet days, the salt moved silently. When the salt was dry, clicks and cracks could be heard 50 m away from the cliff on which the median sight was painted. As the salt was drying, such noises could be heard only when the markers moved upstream (and the salt was generally in tension). When the salt surface was thoroughly dry, the noises were loud and numerous (ten per minute) during all significant movements. Fragments of salt ($< 1 \text{ cm}^3$) fell during particularly large downstream movements (when most of the salt was in compression). Polygonal or rectilinear fractures perpendicular to the vertical or horizontal surfaces of the salt closed as the sun shone on the salt near them and reopened in the evening. Strain gauges bonded across such cracks when they closed recorded strains of several hundred microstrains in directions which changed in response to the position of the sun.
10. By recording temperatures immediately behind increasing thicknesses of dry halite in the sun, we found that the highest temperatures of the

day occurred near 1300 hours on the surface of the salt, near 1500 hours at a depth of 10 cm, and at about 1545 hours at a depth of 20 cm. Just as the daily thermal peak was delayed with depth in the salt, so the thermal peak decreased in value with depth (for example, 44°C at the surface, 25°C at 10 cm, and 20°C at 20 cm, but on different days).

11. S. P. Clark, Jr., *Geol. Soc. Am. Mem.* 97 (1966), p. 75.
12. The slope of the top surface of the salt (α) rarely exceeds 14° , and the thickness (h) is unlikely to be much greater than 50 m. If we use these values and 2.18 g/cm^3 for the density of the salt (ρ) and 982 cm/sec^2 for the gravitational acceleration (g) in the relationship $\tau = \rho gh \sin \alpha$, we find that τ , the shear stress at the bottom of the salt glacier, rarely exceeds 2.5 bars.
13. H. Odé, *Geol. Soc. Am. Spec. Pap.* 88 (1968), p. 543; L. Varo and E. K. S. Passaris, paper presented at the Rock Engineering Symposium, Newcastle University, Newcastle upon Tyne, 1977.
14. We thank the Iranian Geological Survey for providing logistic support and Sir Peter Kent for advice. Financial support was provided by the Royal Society, the Carnegie Trust for the Universities of Scotland, Dundee University, and E. R. Rogers.

7 August 1979; revised 14 January 1980

Sounding the Stratosphere and Mesosphere by Infrared Limb Scanning from Space

Abstract. *Inversion of the measurements obtained by the infrared limb scanner on the Nimbus 6 satellite has demonstrated that the stratospheric and mesospheric temperatures and ozone concentrations may be obtained remotely from space with accuracy and precision comparable to in situ methods. Such global data have many applications in middle atmospheric research and operational temperature sounding.*

The possibility of natural or anthropogenic perturbation of the stratosphere and mesosphere (the middle atmosphere, 15 to 80 km) and especially reduction of the O_3 concentrations have caused considerable concern in recent years (1). This concern over O_3 arises from the threat of increased ultraviolet radiation reaching the earth. Such stratospheric changes could also affect the climate.

In order to provide input parameters for computer models to evaluate these changes and to look for the predicted effects, observations of temperature and trace gas concentrations are required over the globe; this suggests that satellite observations are needed. To be useful, these observations should be accurate, precise, and capable of resolving variations less than a scale height deep.

Most satellite determinations of middle atmosphere temperature structure (for example, results obtained with the selective chopper radiometer and pressure modulated radiometer) and the vertical O_3 distribution (backscatter ultraviolet instruments) thus far have been obtained from measurements made by downward-viewing radiometers and spectrometers (2). Nadir determinations are characterized by low vertical resolution (because the upwelling radiation

comes from effective layers 12 to 20 km deep), the need for more than one sensor to cover a wide range of altitudes, and the inability to measure the vertical distribution of any stratospheric trace gas, except daytime O_3 above 30 km, which requires still another sensor.

Gille (3) pointed out that measurements of infrared radiation emitted by the atmosphere, obtained while the satellite was scanning the earth's horizon or limb, could be inverted to yield day and night vertical distributions of stratospheric and mesospheric temperatures and trace gas concentrations. The advantages of infrared limb scanning include (4) the capability for better vertical resolution (layers approximately 4 km deep) and the capacity to sound for temperatures or trace gases with a single instrument over a wide range of altitudes. The opacity of clouds in the lower atmosphere limits coverage to the upper troposphere and above.

This report presents results from the limb radiance inversion radiometer (LRIR), the first satellite-borne limb scanner. They show that retrievals of temperatures and O_3 concentrations in the stratosphere and mesosphere are not only in good agreement with in situ rocket measurements but also that the quantitative accuracy and precision of limb

scanning are comparable to those of in situ rocket measurements.

The LRIR was fabricated by the Honeywell Electro-Optical Center in Lexington, Massachusetts. It was launched on 12 June 1975 and provided high-quality data for its planned 7-month lifetime. Instrumental details are given elsewhere (5). The fields of view at the horizon (4000 km distant) are 2 km high by 20 km wide. A high signal-to-noise ratio was obtained by cooling mercury-cadmium telluride detectors to 63 K with a two-stage ($\text{CH}_4\text{-NH}_3$) solid cryogenic cooler. Radiometer channels were selected in the bands having strongest atmospheric emission, including two covering the $15\text{-}\mu\text{m}$ bands of CO_2 for temperature determination, and one in the $9.6\text{-}\mu\text{m}$ bands of O_3 . In-flight calibration was effected by having the radiometer "view" cold space and an internal 320 K blackbody every 32 seconds.

Gille and House (4) have described the physical basis of determining temperature as a function of pressure through the use of two regions of the $15\text{-}\mu\text{m}$ CO_2 bands having different opacities. The temperature solution is then used with the measured O_3 channel radiance to determine the O_3 distribution (6).

Examples of typical temperatures and O_3 concentrations are shown by the solid lines in Figs. 1a and 2a, respectively. In situ rocket comparison measurements are shown by the symbols. The altitude coverage is from 15 to 65 km, with vertical resolution adequate to resolve the 6-km temperature structure seen by the rocket (~ 50 km). There is good overall agreement between the temperature determination and the rocket measurement (Fig. 1a), and among all O_3 measurements except near the maximum, where the two rocket techniques show significant differences (Fig. 2a).

In order to assess the LRIR results, their accuracy and precision must be established. The precision, or repeatability, may be determined readily by calculating the standard deviation (σ) of a group of 12 to 16 sequential inversions, at a time and location for which atmospheric variations over the 300 to 400 km covered are minimal. The averages of several determinations are shown by dashed lines in Figs. 1b and 2b. These values result from an "end-to-end" evaluation, which includes the effects of atmospheric variations and data transmission, as well as instrument noise and data processing. For both temperature and O_3 concentration, the repeatability of the LRIR results is similar to (or perhaps slightly better than) that of rocket observations (7, 8).

The accuracy of the LRIR results can be evaluated if one compares them with determinations made by another technique. As there is no absolute standard for stratospheric temperature determina-

tion, comparisons were made with in situ measurements from the meteorological rocket network. The currently used Datasonde has been studied extensively (7); its accuracy is perhaps as good as 1

to 2 K over the altitude region of interest (15 to 65 km). Seventy-eight cases for which great circle distance between the rocket and the satellite overpass were $\leq 2^\circ$ were used. The time differences were up to ± 12 hours for low- and mid-latitude summer and ± 3 hours otherwise. At each of 17 standard levels between 100 and 0.1 mbar, the difference, LRIR retrieval minus rocket, was formed. The mean difference and standard deviation of the mean are also plotted in Fig. 1b.

With few exceptions, the differences between the LRIR and rocket results are not statistically significant and within the Datasonde accuracy. Analysis by latitude shows no systematic trend in the differences. The determination of geostrophic winds depends upon horizontal gradients, which appear to be well preserved in the LRIR temperature retrievals.

Similarly, measurements made by rocket-borne optical and chemiluminescent instruments (8) were used to assess the accuracy of the LRIR O_3 concentrations. The accuracies of both are difficult to determine but are estimated to be about 10 to 15 percent. The mean difference (rocket minus LRIR) of the four comparison cases and its standard deviation are presented in Fig. 2b. Above 30 km the differences are small, not statistically significant, and within rocket instrument accuracy. Below 30 km the rocket values average 1 part per million by volume higher. Work is continuing in an effort to understand this difference.

Thus, for temperature and at least upper level O_3 , an LRIR profile agrees with a coincident rocket measurement about as well as a second rocket would. The immediate conclusion is that infrared limb scanning, with available technology, provides results that are accurate and precise and that reproduce details of the vertical variation in the stratosphere and low mesosphere which cannot now be determined on a global basis in any other way.

Such data provide a wealth of information on the atmosphere from 15 to 65 km; thus many problems can be studied in considerably greater detail than before. For example, the temperatures and geostrophic winds determined from these data will make possible a much more comprehensive study of the vertical propagation of planetary waves. Temperature analyses will facilitate investigations of Kelvin and perhaps Rossby-gravity waves (9) at the equator. Photochemical and radiative balance questions may be examined with the O_3 data.

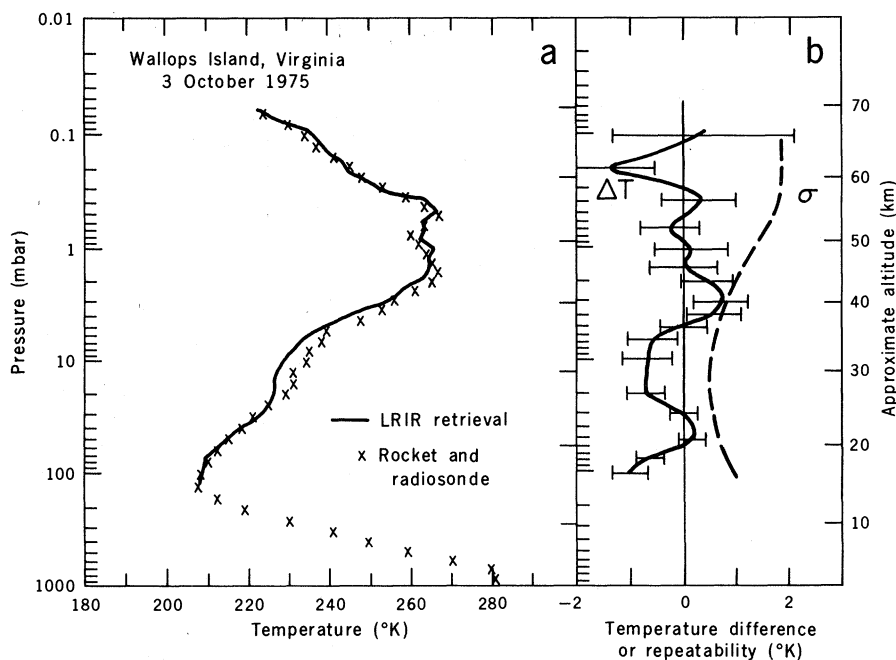


Fig. 1. Results of LRIR temperature retrievals. (a) Typical comparison of LRIR retrieval (solid line) and in situ rocket and radiosonde measurements (symbols). (b) Statistical depiction of repeatability (1σ , dashed line) and accuracy, as evidenced by the mean difference (solid line) between 78 LRIR retrievals and near coincident in situ measurements. Bars show the standard deviation of the mean differences.

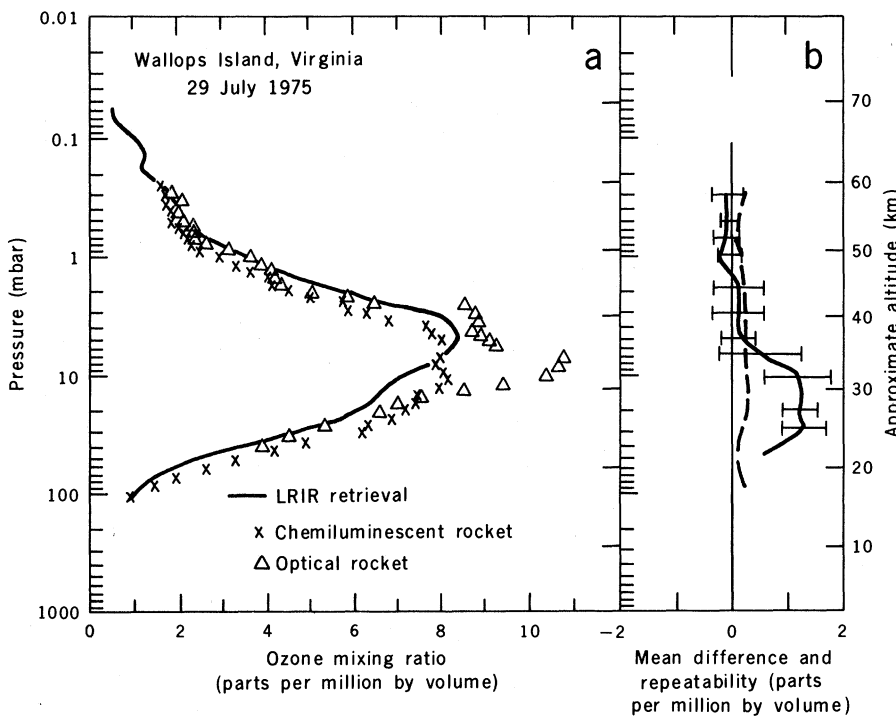


Fig. 2. Results of LRIR O_3 concentrations. (a) Typical comparison of LRIR retrieval (solid line) and in situ rocket measurements (symbols). The mixing ratio is the number of O_3 molecules divided by the number of air molecules in a unit volume, in parts per million by volume. (b) Statistics of O_3 repeatability (1σ , dashed line) and accuracy, as evidenced by the mean differences (solid line) between four LRIR retrievals and near coincident in situ measurements. Bars show the standard deviations of the mean differences.

Perhaps more important, the transport of O₃ by geostrophic winds and changes in the O₃ concentration can be directly observed; this information should contribute significantly to our understanding of the distribution of human impacts on the O₃ layer. Such data may also make possible the first real determination of an anthropogenic effect on the O₃ layer, as a result of a detailed study of the most sensitive region near 40 km (10).

A limb scanner providing temperatures down to the tropopause could be used with a conventional downward-looking temperature sounder to produce considerably improved tropospheric soundings for operational meteorological use. In preliminary calculations, we find that root-mean-square tropospheric temperature errors (~ 2.5 K) can be reduced by up to a factor of 2.

A similar limb scanner on Nimbus 7 has demonstrated the capability to measure the additional trace gases, H₂O, HNO₃, and NO₂ (11). The latter two are the first gases present in the parts-per-billion range to be measured from space.

Thus, infrared limb scanning can provide global observations of the stratosphere and mesosphere with unprecedented vertical resolution, accuracy, and precision. These observations will make possible more quantitative tests of theoretical predictions in those regions and detailed studies of global phenomena such as the interaction of chemistry and dynamics.

JOHN C. GILLE, PAUL L. BAILEY
National Center for Atmospheric
Research, Boulder, Colorado 80307

RICHARD A. CRAIG*
Florida State University,
Tallahassee 32306

FREDERICK B. HOUSE
Drexel University,
Philadelphia, Pennsylvania 19104

GAIL P. ANDERSON
National Center for Atmospheric
Research

References and Notes

1. *Halocarbons: Effects on Stratospheric Ozone* (National Academy of Sciences, Washington, D.C., 1976); *Stratospheric Ozone Depletion by Halocarbons: Chemistry and Transport* (National Academy of Sciences, Washington, D.C., 1979).
2. P. J. Ellis, G. Peckham, S. D. Smith, J. T. Houghton, C. G. Morgan, C. D. Rodgers, E. J. Williamson, *Nature (London)* **228**, 139 (1970); M. D. Austen, J. J. Barnett, P. D. Curtis, C. G. Morgan, J. T. Houghton, G. D. Peskett, C. D. Rodgers, E. J. Williamson, *ibid.* **260**, 594 (1976); D. F. Heath, C. L. Mateer, A. J. Krueger, *Pure Appl. Geophys.* **106-108**, 1238 (1973); J. T. Houghton, *Q. J. R. Meteorol. Soc.* **104**, 1 (1978).
3. J. C. Gille, *J. Geophys. Res.* **73**, 1863 (1968).
4. _____ and F. B. House, *J. Atmos. Sci.* **28**, 1427 (1971).
5. J. C. Gille, P. L. Bailey, F. B. House, R. A. Craig, J. R. Thomas, in *Nimbus 6 Users Guide*, J. E. Sissala, Ed. (NASA Goddard Space Flight Center, Greenbelt, Md., 1975), p. 141.
6. P. L. Bailey and J. C. Gille, in *Remote Sensing*

- of the Atmosphere: Inversion Methods and Applications*, A. L. Fymat and V. E. Zuev, Eds. (Elsevier, Amsterdam, 1978), p. 115; F. B. House and J. C. Gille, in preparation; P. L. Bailey and J. C. Gille, in preparation.
7. F. Schmidlin, in preparation.
 8. E. Hilsenrath, R. L. Coley, P. T. Kirschner, W. Gammill, *NASA Tech. Mem.* 79712 (1979); A. J. Krueger, *Pure Appl. Geophys.* **106-108**, 1272 (1973).
 9. I. Hirota, *J. Atmos. Sci.* **36**, 217 (1979).
 10. P. J. Crutzen, I. S. A. Isaksen, J. R. McAfee, *J. Geophys. Res.* **83**, 345 (1978).
 11. J. M. Russell III and J. C. Gille, *Nimbus 7 Users Guide*, C. Madrid, Ed. (NASA Goddard Space Flight Center, Greenbelt, Md., 1978), p. 263; J. C. Gille, P. L. Bailey, J. M. Russell III, *Philos. Trans. R. Soc. London Ser. A*, in press.

12. We thank the late W. Nordberg for advice in the formative stages of the experiment; the Honeywell staff, especially J. Thomas, J. Bates, R. Blades, and R. Drozewski; and J. Theon, L. Wilson, and the personnel of the Nimbus Project at NASA Goddard Space Flight Center. We thank A. J. Miller, who supplied rocket temperatures, and E. Hilsenrath and A. Krueger, who provided data from chemiluminescent and optical O₃ rockets, respectively, in advance of publication. The program was supported in part by NASA contract NAS5-21652 and work order S 40135B. The National Center for Atmospheric Research is sponsored by the National Science Foundation.
- * Richard A. Craig died on 1 September 1978.

30 November 1979; revised 23 January 1980

Corrections in the Pioneer Venus Sounder Probe Gas Chromatographic Analysis of the Lower Venus Atmosphere

Abstract. Misidentification of two peaks from the Pioneer Venus sounder probe gas chromatograph (SPGC), also formerly known as the LGC, gave rise to quantitative errors in the abundances of oxygen, argon, and carbon monoxide. The argon abundance is estimated at 67 parts per million and that of carbon monoxide at 20 parts per million. At this time, no estimates for the oxygen abundance can be made.

We reported earlier on the compositional analysis of the lower atmosphere of Venus (1). We report here a revised compositional analysis derived from simulation studies and further chromatographic comparison (Table 1). This composition differs from that published earlier because we had misidentified the Ar peak as O₂ and the CO peak as Ar. This consequently gave rise to the quantitative errors because response factors are different for each component analyzed. An equivocal presence of O₂, revised values for Ar, and an estimation of CO (instead of an upper limit in the lower atmosphere of Venus) are shown in Table 1. The misidentifications of peaks were caused by assuming that the reten-

tion times were sufficient for identification. This conclusion was reasonable as derived from Table 2, where retention times from the flight data were matched with those of known calibration gas standards obtained before flight. The largest difference was in Freon 14, which had a retention time of 24 seconds less in the flight data than in the calibration tests. We assumed that the temperature of the column rose during the later stages of the third analysis and did not put any credence on the shortened retention time of the added Freons. We have since found that the short retention times for all gases were caused by higher mass flow rates in the column.

We discovered the error after com-

Table 1. Revised atmospheric composition of Venus as measured by the SPGC.

Gas	Flight sample		
	1	2	3
	Concentration (%) ± confidence interval*		
CO ₂	95.4 ± 2.0	95.9 ± 5.8	96.4 ± 1.0
N ₂	4.60 ± 0.14	3.54 ± 0.04	3.41 ± 0.01
H ₂ O	< 0.06	0.519 ± 0.068	0.135 ± 0.015
	Concentration (ppm) ± confidence interval*		
O ₂	?	?	?
CO	32.2 $\left\{ \begin{array}{l} + 61.7 \\ - 22.2 \end{array} \right.$	30.2 ± 18.0	19.9 ± 3.1
Ar	60.5 ± 46.8	63.8 ± 13.6	67.2 ± 2.3
Ne	< 8	10.6 $\left\{ \begin{array}{l} + 31.6 \\ - 9.6 \end{array} \right.$	4.31 $\left\{ \begin{array}{l} + 5.54 \\ - 3.91 \end{array} \right.$
SO ₂	< 600	176 $\left\{ \begin{array}{l} + 2000 \\ - 0 \end{array} \right.$	185 $\left\{ \begin{array}{l} + 350 \\ - 155 \end{array} \right.$
Altitude† (km)	51.6	41.7	21.6
Pressure‡ (bars)	0.698 ± 0.140	2.91 ± 0.17	17.8 ± 0.2

*Confidence intervals are calculated from the calibration data acquired during the test and are determined to 3σ (σ is the standard deviation) (8). †Altitudes are interpolated from data provided by A. Seiff and represent the altitude at the time of sample injection. ‡Atmospheric pressure at the time of injection as determined by the SPGC from the sum of all measured components.